OncoTargets and Therapy

Dovepress
open access to scientific and medical research

Open Access Full Text Article

ORIGINAL RESEARCH

Protein kinase C-iota-mediated glycolysis promotes non-small-cell lung cancer progression

This article was published in the following Dove Press journal:
OncoTargets and Therapy

Liu Liu[1,*]
Bei Lei[1,*]
Lihua Wang[1]
Cheng Chang[1]
Hao Yang[2]
Jianjun Liu[3]
Gang Huang[1–3]
Wenhui Xie[1]

[1]Department of Nuclear Medicine, Shanghai Chest Hospital, Shanghai Jiao Tong University, Shanghai, People's Republic of China; [2]Shanghai Key Laboratory for Molecular Imaging, Shanghai University of Medicine and Health Sciences, Shanghai, People's Republic of China; [3]Department of Nuclear Medicine, Renji Hospital, School of Medicine, Shanghai Jiao Tong University, Shanghai, People's Republic of China

*These authors contributed equally to this work

Purpose: To determine whether protein kinase C-iota (PKC-iota) is associated with glucose metabolism in non-small-cell lung cancer (NSCLC) and whether its regulatory effect on metabolic and biological changes observed in NSCLC can be mediated by glucose transporter 1 (GLUT1).

Patients and methods: Forty-five NSCLC patients underwent combined ^{18}F-fludeoxyglucose (^{18}F-FDG) positron emission tomography and computed tomography (PET/CT) before surgery, and another eighty-one NSCLC patients were followed-up for 1–91 months after tumor resection. The rate of glucose metabolism in NSCLC was quantified by measuring the maximum standardized uptake value (SUVmax) by ^{18}F-FDG PET/CT. PKC-iota and GLUT1 in NSCLC were detected by immunostaining. In vitro, PKC-iota was knocked down, whereas GLUT1 was silenced with or without PKC-iota overexpression to identify the role of PKC-iota in glycolysis. Spearman's rank correlation coefficient was used in the correlation analysis. Kaplan-Meier analysis was used to assess survival duration.

Results: There was a positive relationship between PKC-iota expression and SUVmax in NSCLC (r=0.649, P<0.001). PKC-iota expression also showed a positive relationship with GLUT1 in NSCLC tissues (r=0.686, P<0.001). Patients whose NSCLC tissues highly co-expressed PKC-iota and GLUT1 had worse prognosis compared with patients without high co-expression of PKC-iota and GLUT1. In vitro, PKC-iota silencing significantly decreased the expression of GLUT1 and inhibited glucose uptake and glycolysis; c-Myc silencing restrained PKC-iota-mediated GLUT1 elevation; GLUT1 knockdown remarkably suppressed PKC-iota-mediated glycolysis and cell growth.

Conclusion: In NSCLC, the rate of glucose metabolism was positively correlated with PKC-iota expression. PKC-iota increased glucose accumulation and glycolysis by upregulating c-Myc/GLUT1 signaling and is thus involved in tumor progression.

Keywords: protein kinase C-iota, glucose transporter 1, ^{18}F-fludeoxyglucose, glycolysis, non-small-cell lung cancer

Introduction

Lung cancer is the most common and fatal malignancy worldwide; non-small-cell lung cancer (NSCLC) accounts for ~83% of lung cancers.[1,2] Similar to many other tumors, NSCLC involves in not only uncontrolled cell proliferation but also energy metabolic reprogramming.[3,4] The most prominent metabolic characteristic of these tumors is the Warburg effect, which manifests as avid glucose consumption and lactic acid production, even in the presence of oxygen (aerobic glycolysis).[5] In recent years, due to an in-depth understanding of tumor energy metabolism, glycolysis has been recognized as an attractive target for tumor therapy.[6] Thus, in NSCLC, the search for new molecular markers involved in glycolysis is crucial for exploring innovative therapeutic anti-tumor strategies.

Correspondence: Gang Huang; Wenhui Xie
Department of Nuclear Medicine, Shanghai Chest Hospital, Shanghai Jiao Tong University, 241 Huaihai West Road, Shanghai 200030, People's Republic of China
Tel +86 212 220 0000
Fax +86 212 220 0000
Email shxknuclear@126.com; huanggang0311@163.com

submit your manuscript | www.dovepress.com
DovePress
http://doi.org/10.2147/OTT.S207211

Protein kinases C (PKCs) are widely implicated in cell proliferation control, with positive or negative effects on tumor growth.[7–9] PKC-iota is the first PKC reported as an oncogenic enzyme in NSCLC,[10] and contributes to tumor progression via immune suppression, cell cycle deregulation, and pericellular degradation of the extracellular matrix.[11–13] Although other PKCs were reported to directly phosphorylate glucose transporter 1 (GLUT1), which is the key rate-limiting carrier in charge of glucose transportation, thereby promoting its activation and the transport of glucose across plasma membranes,[14] the regulatory effect of PKC-iota on GLUT1 is not yet well established. Whether PKC-iota is involved in glucose metabolism in tumors remains unknown.

At the molecular level, excessive GLUT1 activation directly upregulates glucose accumulation in cancer cells to ensure energy supply, triggering uncontrolled cancer cell growth.[15,16] GLUT1 is overexpressed in multiple types of cancer, including NSCLC.[17–21] The trans-glucose function of GLUT1 depends on its membrane localization.[22,23] In addition to intrinsic activation and post-translational stabilization,[24,25] GLUT1 can also be transcriptionally upregulated by c-Myc, hypoxia-inducible factor-1 alpha (HIF-1a), or oculis homeobox 1 (SIX1).[15,26,27] Recently, c-Myc expression was proven to be controlled by PKC-iota in cancer cells,[28] which led us to hypothesize that PKC-iota may also regulate GLUT1 expression, thus inducing glucose uptake and subsequent glycolysis in NSCLC.

In vivo, combined ^{18}F-fludeoxyglucose (^{18}F-FDG) positron emission tomography and computed tomography (PET/CT) can indirectly evaluate the glucose metabolic rate of cancer cells by measuring standardized uptake value (SUV),[29] and this approach is widely used in tumor diagnosis. In this study, we combined ^{18}F-FDG PET/CT examinations with immunohistochemical (IHC) assays to determine whether PKC-iota is associated with glucose metabolism in NSCLC. We also sought to elucidate the mechanisms of PKC-iota involved in glucose metabolism and to confirm the key role of GLUT1 in PKC-iota–mediated progression.

Materials and methods

Study population

The institutional ethics committee of the Shanghai Chest Hospital and Renji Hospital, which are affiliated with Shanghai Jiao Tong University, approved this study, and written informed consent was obtained from all participants included in the study, according to the Declaration of Helsinki. This study was performed without industrial sponsorship or support.

For this retrospective study, we identified forty-five patients with NSCLC who had undergone ^{18}F-FDG PET/CT 2–4 weeks before tumor resection between June and July 2017 at Shanghai Chest Hospital, including 30 men (mean age, 59.0 years; age, 39–75 years) and 15 women (mean age, 57.9 years; age, 48–68 years). The inclusion criteria were as follows: NSCLC confirmed via pathologic examination of surgical specimens; and availability of age, gender and tissue specimens for IHC staining. Patients with primary lesions smaller than 1.0 cm, local necrosis, and ground-glass nodules were excluded from the study.

We also identified another eighty-one patients with NSCLC, including 58 men (mean age, 64.0 years; age, 35–86 years) and 23 women (mean age, 63.9 years; age, 51–83 years), who had undergone tumor resection at Shanghai Chest Hospital and Renji Hospital between 2008 and 2013 and who were followed-up until September 2016 (from 1 to 91 months after surgery, with a median time of 47 months). The inclusion criteria were as follows: NSCLC confirmed via pathologic examination of surgical specimens; and availability of age, gender, smoking history, tumor length (the largest diameter), nodal metastasis, TNM stage, and histologic subtype. Staging was performed postoperatively and assessed according to the International Union Against Cancer (UICC) lung cancer TNM staging standard of 2017. No smoking meant never smoking or smoking fewer than 100 cigarettes in a lifetime.

PET/CT examination

^{18}F-FDG PET/CT was performed after fasting for 8 h and 60 min after intravenous administration of ^{18}F-FDG (5–10 mCi, depending on patient weight). The blood glucose levels, measured just before tracer administration, were <8.0 mmol/L in all patients. Imaging was performed with a combined PET/CT device (Biograph mCT; Siemens, Erlangen, Germany). CT scans were acquired using the following parameters: 16×1.2 mm collimation (140 kV, 80 mAs), 5 mm slice, 0.5 s rotation time, and 0.8 pitch. Immediately after CT, PET was performed with an acquisition time of 3 min per bed position and six to eight bed positions per patient, depending on patient height. CT data were used for attenuation correction. Axial, sagittal, and coronal images were examined using Syngo software and then transferred in DICOM format to a Syngo workstation

(Siemens). A region of interest (ROI) was placed over the primary tumor by two experienced nuclear medicine physicians to measure each SUVmax, and discrepancies between their assessments were resolved by consensus through discussion. The nuclear medicine physicians were blinded to the IHC analysis. SUVmax was calculated with the most commonly applied formula: SUVmax = maximum pixel activity/(injected dose/body weight).

Immunohistochemistry

The experiment using human tissues was approved by the Human Assurance Committee of Shanghai Chest Hospital and Renji Hospital. Formalin-fixed paraffin sections (thickness: 5 μm) were used for IHC staining with anti-PKC-iota rabbit polyclonal antibody (Proteintech Group, IL, USA) or anti-GLUT1 mouse monoclonal antibody (Abcam, CBG, UK), followed by incubation with HRP-conjugated goat anti-rabbit IgG (Cell Signaling, MA, USA) or HRP-conjugated goat anti-mouse IgG (Cell Signaling), respectively. A 3,3′-diaminobenzidine (DAB) chromogen substrate solution was used to visualize the results.

PKC-iota and GLUT1 expression in NSCLC tissues was scored blindly and independently by two experienced pathologists, and discrepancies between their assessments were resolved by consensus through discussion. Staining frequency (0=0%, 1=1–9%, 2=10–49%, 3=50–100%) and intensity (0= negative, 1= weak, 2= moderate and 3= strong staining) scores were multiplied to calculate the overall staining score (OSS). An OSS of 0–3 was considered low expression, whereas a score of 4–9 was considered high expression.

Cell culture, reagents, plasmids, and siRNA

A549, PC9, H1299, H1975, and H1650 cells were purchased from the Cell Bank of the Type Culture Collection of the Chinese Academy of Sciences and were cultured at 37 °C under 5% CO_2 in Dulbecco's Modified Eagle Medium (DMEM) (Gibco, NY, USA) supplemented with 10% heat-inactivated fetal bovine serum (FBS) (HyClone, UT, USA), 100 mg/mL penicillin (Gibco), and 100 mg/mL streptomycin sulfate (Gibco). Lipofectamine 2000 reagent (Invitrogen, CA, USA) was used for transient transfection following the manufacturer's instructions.

Polymerase chain reaction (PCR)-amplified and DNA sequencing-verified human *protein kinase C-iota* (*PRKCI)* was cloned into PCDNA3.1-MCS2. The primers used in the *PRKCI* clone are as follows: forward primer: 5′-CCAAGCTGGCTAGCGGAATTCGCCACCATGCCGACCCAGAGGGACAG-3′; reverse primer: 5′-CAAGCTTGCTCGAGTCGGATCCTCACTTGTCGTCATCGTCCTTGTAGTCG-3′.

The siRNA sequences used are as follows: Si PKC-iota: sense, 5′-GCAAUGAGGUUCGAGACAUTT-3′, anti-sense, 5′-AUGUCUCGAACCUCAUUGCTT-3′; Si GLUT1: sense, 5′-UGAUGUCCAGAAGAAUAUU-3′, anti-sense, 5′-ACUACAGGUCUUCUUAUAA-3′; Si c-Myc: sense: 5′-TGCTCCATGAGGAGACACC-3′; anti-sense: 5′-CTTTTCCACAGAAACAACATCG-3′.

Glucose metabolism assay

^{18}F-FDG uptake was used to determine cellular glucose uptake capacity. Cells were seeded into 12-well culture plates and then cultured in 1 mL of Roswell Park Memorial Institute 1640 (RPMI-1640) (Gibco) containing 4 μCi ^{18}F-FDG for 1 h at 37 °C. The gamma counter was used to assay ^{18}F-FDG radioactivity in whole-cell lysates. Lactate production was assayed with a lactate assay kit (Lactate Assay Kit; Microdialysis, STO, SWE) according to the manufacturer's protocol. All experiments were independent of each other and performed in triplicate, and the readouts were normalized to the corresponding protein quantities by using a protein assay kit (BCA Protein Assay Kit; Beyotime, Shanghai, China).

Immunoblotting analyses

Cells were lysed in radioimmunoprecipitation assay (RIPA) buffer before sodium dodecyl sulfate polyacrylamide gel electrophoresis, then transferred to polyvinylidene fluoride membranes (GE Healthcare, Bucks, UK) and probed with the indicated primary and horseradish peroxidase (HRP)-conjugated secondary antibodies (Santa Cruz, CA, USA). The chemiluminescent HRP substrate (Millipore, MA, USA) was used to visualize antibody binding. Anti-PKC-iota rabbit polyclonal antibody (Proteintech Group), anti-GLUT1 rabbit polyclonal antibody (Abcam), anti-c-Myc rabbit monoclonal antibody (Abcam), and anti-β-Tubulin mouse polyclonal antibody (Proteintech Group) were used.

Gene expression analysis

Total RNA was isolated from cells by using an E.Z.N. A total RNA Kit I (Omega Bio-tek, GA, USA). cDNA was synthesized using a Primer Script RT reagent Kit (Takara,

Otsu, Japan). Real-time PCR was performed according to the protocol of the SYBR Premix Ex Taq kit (Takara) and using a StepOnePlus Real-Time PCR System (Applied Biosystems, USA). The fluorescence data of the detected genes were normalized to cyclophilin B (CB, forward primer: 5′- AGATGTAGGCCGGGTGATCT-3′, reverse primer: 5′- CCGCCCTGGATCATGAAGTC-3′) expression by using the $2^{-\Delta\Delta CT}$ method. The following primers were also used to detect relative genes: *PRKCI* gene expression: forward primer: 5′-GGCTGCATTCTTGCT TTCAGA-3′, reverse primer: 5′-CCAAAAATATGA AGCCCAGTAATCA-3′; solute carrier family 2 member 1 (*SLC2A1)* gene expression: forward primer: 5′-ATTGGCTCCGGTATCGTCAAC-3′; reverse primer: 5′-GCTCAGATAGGACATCCAGGGTA-3′; *MYC*: forward primer: 5′-ACACCCTTCTCCCTTCG-3′; reverse primer: 5′-CCGCTCCACATACAGTCC-3′; *HIF-1a*: forward primer: 5′-CATGTGACCATGAGGAAATG-3′; reverse primer: 5′-GTTGGTTACTGTTGGTATCATA-3′; *SIX1*: forward primer: 5′-ACAAGAACGAGAGCGTACTCA-3′; reverse primer: 5′-GCTCTCGTTCTTGTGCAGGT-3′.

Immunofluorescent staining

Cells were moved to glass coverslips for 24 h before staining. The cells were then fixed in 4% polyoxymethylene (PFA, pH 7.4) for 30 min at 37 °C, permeabilized with 0.5% Tween-20 for 10 min, and then blocked with-goat serum for 30 min at 37 °C. Cells were then incubated with primary antibodies (GLUT1 mouse monoclonal antibody [Abcam] and Na,K-ATPase α1 rabbit monoclonal antibody [Cell Signaling]) overnight at 4 °C. Secondary antibodies labeled with Alexa Fluor 488 (green) or Alexa Fluor 594 (red) (Invitrogen, CA, USA) were added and incubated for 1 h at 37 °C. Nuclei were stained using 4,6-diamidino-2-phenylindole (DAPI, Invitrogen). Immunofluorescence (IF) was visualized under a confocal laser-scanning microscope (CLSM 510) (Carl Zeiss, Jena, Germany).

Cell growth assay

For the cell proliferation assay, cells were plated on 24-well plates (5000 cells/well × wells) and counted at different time points after transfection. For the cell motility assay, cells were seeded into 12-well plates for confluence before a linear wound was made; the wounded monolayers were photographed at 0 and 24 h after wounding. For the cell invasion assay, suspended cells (1×10^5/well) were transferred to the upper chamber with a Matrigel-coated membrane in a 24-well plate with 8-μm pore size chamber inserts (Corning, NY, USA). After 24 h, the invading cells that moved to the bottom surface of the chamber were fixed with 4% formalin and stained with 0.1% crystal violet before imaging and counted in 5 random fields.

Data analysis

Data were analyzed using GraphPad Prism 6 (GraphPad Software, San Diego, CA) or SPSS 19.0 (SPSS, IL, USA). Quantitative data were expressed as the mean ± standard deviation (SD) values of at least three independent experiments. Statistical differences between two groups were assessed by the paired or unpaired two-tailed *t*-test. The chi-squared test was used for rate comparisons. Spearman rank correlation was used in correlation analysis. Kaplan-Meier analysis was used in the survival duration assay. Differences identified with * (denoting a P-value <0.05) or ** (denoting a P-value <0.005) were all considered statistically significant.

Results

Association of PKC-iota with SUVmax and GLUT1 expression in primary NSCLC tissues

To understand the correlation between PKC-iota and glucose metabolism in NSCLC, we assessed the relationship of PKC-iota protein expression and SUVmax, the most commonly used parameter of ^{18}F-FDG PET/CT to determine the tumor glucose metabolic rate,[29] in 45 NSCLC tissues from patients who underwent ^{18}F-FDG PET/CT 2–4 weeks before surgery. Lesions smaller than 1.0 cm and ground-glass nodules were excluded because of the partial volume effect of PET; tissues with local pathologically diagnosed necrosis were also excluded to maintain the relative homogeneity of tumors. PKC-iota was mainly detected in the cytoplasm of cancer cells, whereas its expression was relatively weak in the membrane and nucleus (Figure 1A and B). Interestingly, an apparent positive relationship was noted between PKC-iota staining scores and SUVmax values (r=0.649, P<0.001) (Figure 1A and B).

We also detected GLUT1 protein expression in NSCLC tissues. GLUT1 was mainly expressed in the membrane, with weak and diffuse staining in the cytoplasm and nucleus (Figure 1A and B). A positive relationship between GLUT1 and PKC-iota protein levels was also observed in our study

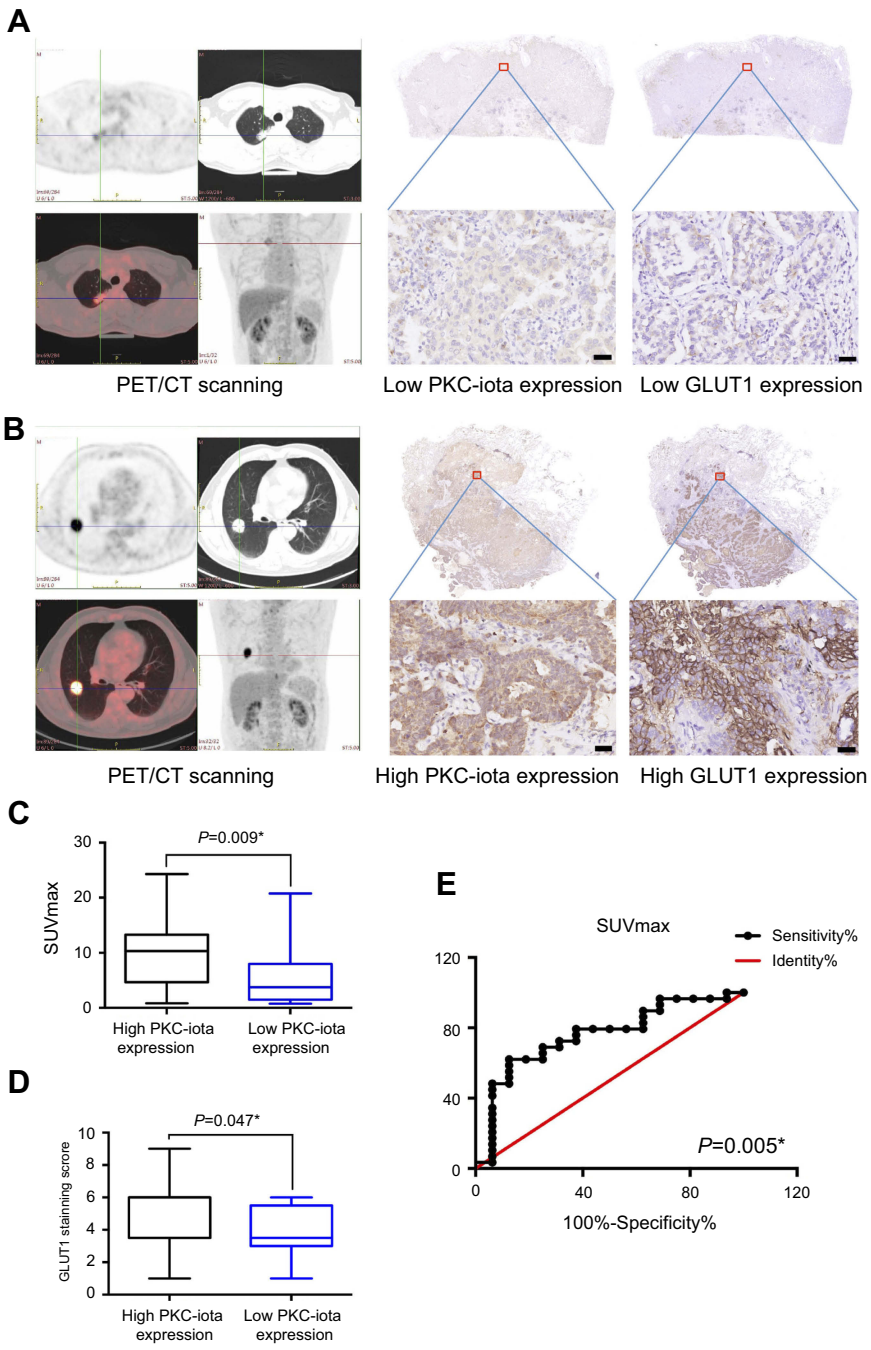

Figure 1 PKC-iota is associated with GLUT1 and SUVmax in primary NSCLC. (**A, B**) Images of ^{18}F-PET/CT scanning, H/E staining, PKC-iota staining, and GLUT1 staining of primary NSCLC tissues of a patient (**A**) with relatively low ^{18}F-FDG uptake (SUVmax =3.59) and low PKC-iota and GLUT1 co-expression (scale bar: 25 μm) and another patient (**B**) with relatively high ^{18}F-FDG uptake (SUVmax =16.47) and high PKC-iota and GLUT1 co-expression (scale bar: 25 μm). (**C**) NSCLC tissues with high PKC-iota expression (10.07±1.09) accumulated much more ^{18}F-FDG than tissues with low PKC-iota expression (5.28±1.28). (**D**) NSCLC tissues with high PKC-iota expression (5.03 ±0.41) expressed much more GLUT1 than tissues with low PKC-iota expression (3.75±0.40). (**E**) ROC curve analysis of SUVmax for predicting high PKC-iota expression. With a SUVmax cutoff value of 8.38, the sensitivity and specificity for high PKC-iota expression prediction were 62.07% and 87.50%, respectively (*P*=0.005; area under the ROC curve: 0.757; 95% confidence interval: 59.11% to 89.21%).

(r=0.587, *P*<0.001). Moreover, when NSCLC tissues were divided into high (OSS >3) and low (OSS ≤3) PKC-iota expression groups, tissues with high PKC-iota expression accumulated much more ^{18}F-FDG and expressed much more GLUT1 than those with low PKC-iota expression (Figure 1C and D). Receiver operating characteristic (ROC) analysis also revealed that an SUVmax value of 8.38 was optimal for predicting high PKC-iota expression in primary NSCLC tissues (*P*=0.005; sensitivity: 62.07%; specificity: 87.50%) (Figure 1E).

PKC-iota knockdown inhibits glycolysis and GLUT1 expression

To investigate the role of PKC-iota in glycolysis in lung cancer, we used siRNA to knock down endogenous PKC-iota and assessed ^{18}F-FDG uptake and lactic acid production in two lung cancer lines with different basal PKC-iota and GLUT1 levels (Figure S1). Notably, PKC-iota knockdown clearly decreased cellular ^{18}F-FDG uptake and glycolysis (Figure 2A and B). At the protein level, PKC-iota silencing decreased GLUT1 expression in NSCLC cells (Figure 2C). We also observed changes in the mRNA levels of *SLC2A1*, the gene encoding GLUT1, and confirmed that the decrease in GLUT1 expression induced by PKC-iota silencing occurred at the transcriptional level (Figure 2D). We then assessed the membrane localization of GLUT1, which is essential for its activation, via IF staining; a Na/K-ATPase α1 antibody was used to label the cell membrane. The results showed that PKC-iota silencing apparently decreased both GLUT1 protein expression and membrane localization (Figure 2E). These data prove that PKC-iota promotes GLUT1 expression at the transcription level and increases GLUT1 activation in NSCLC cells.

PKC-iota upregulates GLUT1 expression via modulating c-Myc expression

To investigate the mechanism of PKC-iota regulation of GLUT1 gene *(SLC2A1)* transcription, we also detected the gene expression of *MYC, HIF-1a* and *SIX1*, the three key transcriptional factors regulating GLUT1 in A549 cells, wherein endogenous PKC-iota was knocked down. The data showed that PKC-iota (*PRKCI*) silencing markedly decreased the mRNA levels of *MYC* and *SLC2A1*, whereas *HIF-1a* and *SIX1* changed only slightly (Figure 3A). Moreover, we found that exogenous PKC-iota could increase the protein levels of GLUT1 and c-Myc in H1650 cells, a lung cancer line with relatively low basal GLUT1 expression, which was impaired by c-Myc silencing (Figure 3B). These data prove that PKC-iota promotes GLUT1 expression via modulating c-Myc expression.

GLUT1 knockdown blocks PKC-iota–mediated glycolysis and cell growth

To determine whether GLUT1-related glycolysis is involved in PKC-iota-induced tumor growth, we used siRNA to knock down endogenous GLUT1 in NSCLC cells with or without exogenous PKC-iota expression to observe changes in glucose metabolism and growth in lung cancer cells. We found that exogenous PKC-iota increased GLUT1 protein expression, ^{18}F-FDG uptake, and glycolysis in NSCLC, which was markedly inhibited by GLUT1 knockdown (Figure 4A–C). Furthermore, the cell growth assay showed that GLUT1 silencing could also restrain the cell proliferation, migration, and invasion induced by exogenous PKC-iota overexpression (Figure 5A–C). Based on these in vitro results, GLUT1-related glycolysis can be considered essential for PKC-iota-mediated malignant growth of lung cancer cells.

Relationship between PKC-iota and GLUT1 expression and clinicopathological characteristics of NSCLC

To further elucidate the indispensability of GLUT1 in PKC-iota–related progression of NSCLC, we analyzed PKC-iota and GLUT1 expression in NSCLC tissues from 81 patients for whom detailed clinicopathological parameter data were available. These patients were followed postoperatively for 1–91 months by IHC staining. As reported,[30,31] the protein levels of PKC-iota and GLUT1 were positively correlated with a large tumor size, nodal metastasis, and late TNM stage of NSCLC, whereas no significant differences in PKC-iota and GLUT1 expression were found in terms of age, sex, or smoking history (Table 1). We also observed relatively lower PKC-iota and GLUT1 expression levels in adenocarcinoma (ADC) cells than in squamous carcinoma (SQCC) cells (Table 1).

In addition, the Kaplan-Meier survival curve showed that, when compared with patients without PKC-iota and GLUT1 high coexpression, patients whose primary NSCLC tissues highly co-expressed PKC-iota and GLUT1 had worse prognosis (Figure 6). The median survival time of patients whose tumors had different PKC-iota and GLUT1 levels were 33 (PKC-iota and GLUT1 high coexpression), 66 (high PKC-iota and low GLUT1 expression), 66.5 (low PKC-iota and low GLUT1 expression), and 78 (low PKC-iota and high GLUT1 expression) months, respectively. Thus, our results suggest the pivotal role of GLUT1 in PKC-iota-mediated tumor progression.

Discussion

Lung cancer is the most common form of malignancy worldwide. Although the application of many targeted drugs tends to improve patient outcomes,[32–34] lung cancer

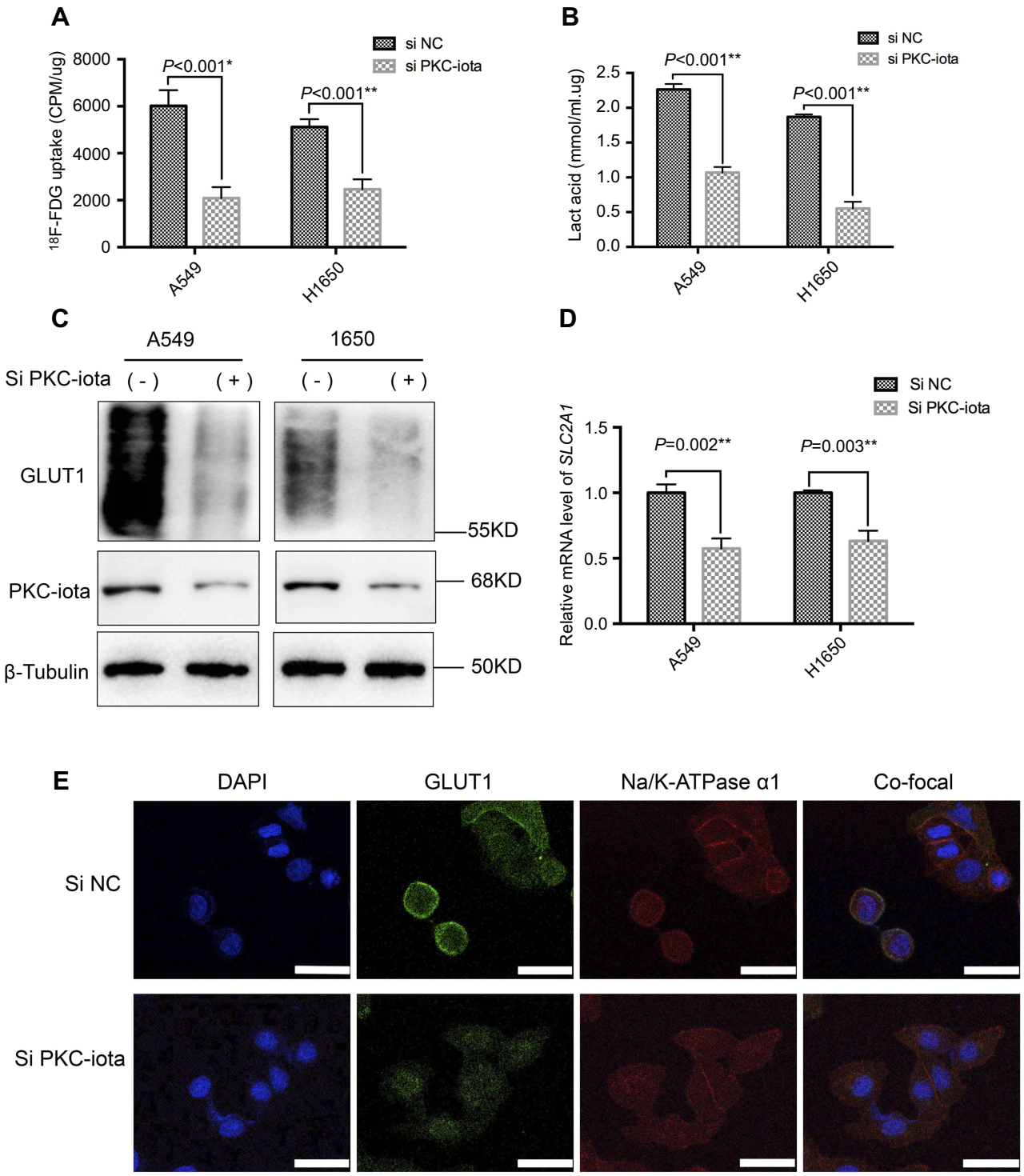

Figure 2 PKC-iota knockdown reduces ^{18}F-FDG uptake and GLUT1 expression. (**A**) A549 and H1650 cells were transfected with Si NC or Si PKC-iota for 72 h, after which time ^{18}F-FDG uptake of the indicated cells was detected (CPM: counts per minute). (**B**) A549 and H1650 cells were transfected with Si NC or Si PKC-iota for 72 h, after which time lactic acid production of the indicated cells was detected. (**C**) A549 and H1650 cells were transfected with Si NC or Si PKC-iota for 72 h. Then, the cell lysates were immunoblotted with antibodies against PKC-iota and GLUT1. β-Actin served as the loading control. (**D**) A549 and H1650 cells were transfected with Si NC or Si PKC-iota for 36 h. The mRNA levels of *SLC2A1* were analyzed by real-time PCR. (**E**) A549 cells were transfected with Si NC or Si PKC-iota for 72 h before IF staining. Staining for DAPI (blue), GLUT1 (green), Na/K-ATPase α1 (red) and the overlays of three channels (the membrane localization of GLUT1 are shown in yellow) are shown in the first, second, third, and fourth lines, respectively (scale bar, 25 μm).

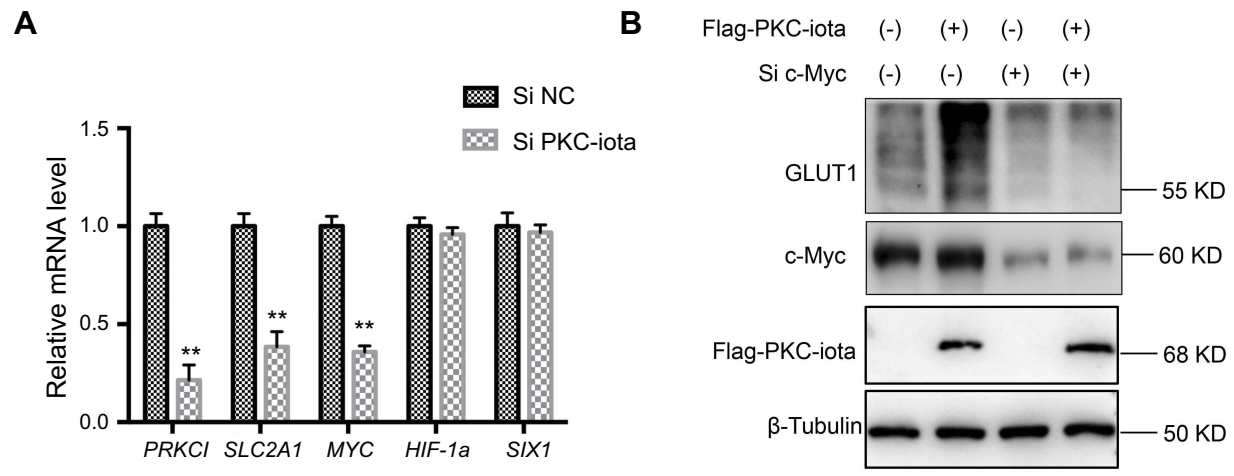

Figure 3 PKC-iota regulates GLUT1 via modulating c-Myc expression. (**A**) A549 cells were transfected with Si NC or Si PKC-iota for 36 h. The mRNA levels of the indicated genes were analyzed by real-time PCR. **means a *P*-value <0.005. (**B**) H1650 cells were co-transfected with Flag-PKC-iota (or empty vector) and Si c-Myc (or Si NC) for 72 h. Then, the cell lysates were immunoblotted with the indicated antibodies. β-Tubulin served as the loading control.

is still the leading cause of cancer-related death. Recent evidence suggests that increased glucose accumulation is associated with NSCLC progression.[31,35–37] Persistent glucose uptake and subsequent aerobic glycolysis are essential to meet the energy and macromolecular biosynthesis demands of cancer cells.[5] Understanding the mechanisms of glycolysis in NSCLC helps to develop effective metabolic-targeting and monitoring strategies. In this study, we identified the oncogenic enzyme PKC-iota as a new molecular marker involved in glucose metabolism in NSCLC. More importantly, we confirmed that PKC-iota promoted glycolysis via upregulating c-Myc/GLUT1 signaling, which might be essential for tumor progression.

Human PKCs comprise three types: classic (cPKC: alpha, beta, and gamma), novel (nPKC: delta, epsilon, eta, and theta), and atypical (aPKC: zeta and iota).[7] PKC-iota is an atypical PKC involved in the malignant growth of multiple types of cancer.[38–40] PKC-iota overexpression in NSCLC was first observed in 2005 and was related to the short survival time of NSCLC patients.[10] The modulatory effect of PKC-iota on the glycolysis-related transcription factor c-Myc led us to probe its possible role in tumor glucose metabolism.[28] As expected, we observed a positive relationship between PKC-iota protein levels and glucose metabolic rates in NSCLC via IHC and ^{18}F-FDG PET/CT. In addition, in vitro data showed that PKC-iota silencing restrained ^{18}F-FDG uptake and glycolysis, whereas exogenous PKC-iota upregulated both ^{18}F-FDG uptake and glycolysis in lung cancer cells, thus proving the involvement of PKC-iota in tumor glycolysis and suggesting the need for glycolysis-targeting therapies for NSCLC patients with PKC-iota overexpression.

As an enzyme, PKC-iota is involved in tumor growth via post-translational modification of other proteins.[41] For example, PKC-iota can phosphorylate Sex determining region Y box 2 to drive tumorigenesis in NSCLC;[38] PKC-iota-induced phosphorylation of YAPI can increase its nuclear localization and transcriptional activity to promote ovarian cancer progression.[42] PKC-iota can also directly phosphorylate FoxO1, a transcription factor regulating the *MYC* gene, thus controlling the expression of c-Myc,[28] a key transcription factor that stimulates tumor glycolysis by directly transactivating GLUT1 and other glycolysis-related genes.[43] In the present study, we proved that PKC-iota also regulated the expression of GLUT1 via modulating c-Myc signaling: PKC-iota silencing decreased both GLUT1 gene and protein expression levels and reduced the levels of active membrane-locating GLUT1, whereas exogenous PKC-iota elevated the protein expression of GLUT1; PKC-iota silencing also decreased *MYC* expression, whereas *HIF-1a* and *SIX1*, two other transcription factors regulating GLUT1, remained virtually unchanged; exogenous PKC-iota elevated the protein levels of GLUT1, which was inhibited by c-Myc silencing. Moreover, GLUT1 silencing suppressed PKC-iota-mediated ^{18}F-FDG accumulation and subsequent glycolysis in NSCLC cells. Taken together, we confirmed that PKC-iota regulated glycolysis via c-Myc/GLUT1 signaling; the regulatory effect of PKC-iota on GLUT1 occurred at the transcriptional level; the most likely reason for the

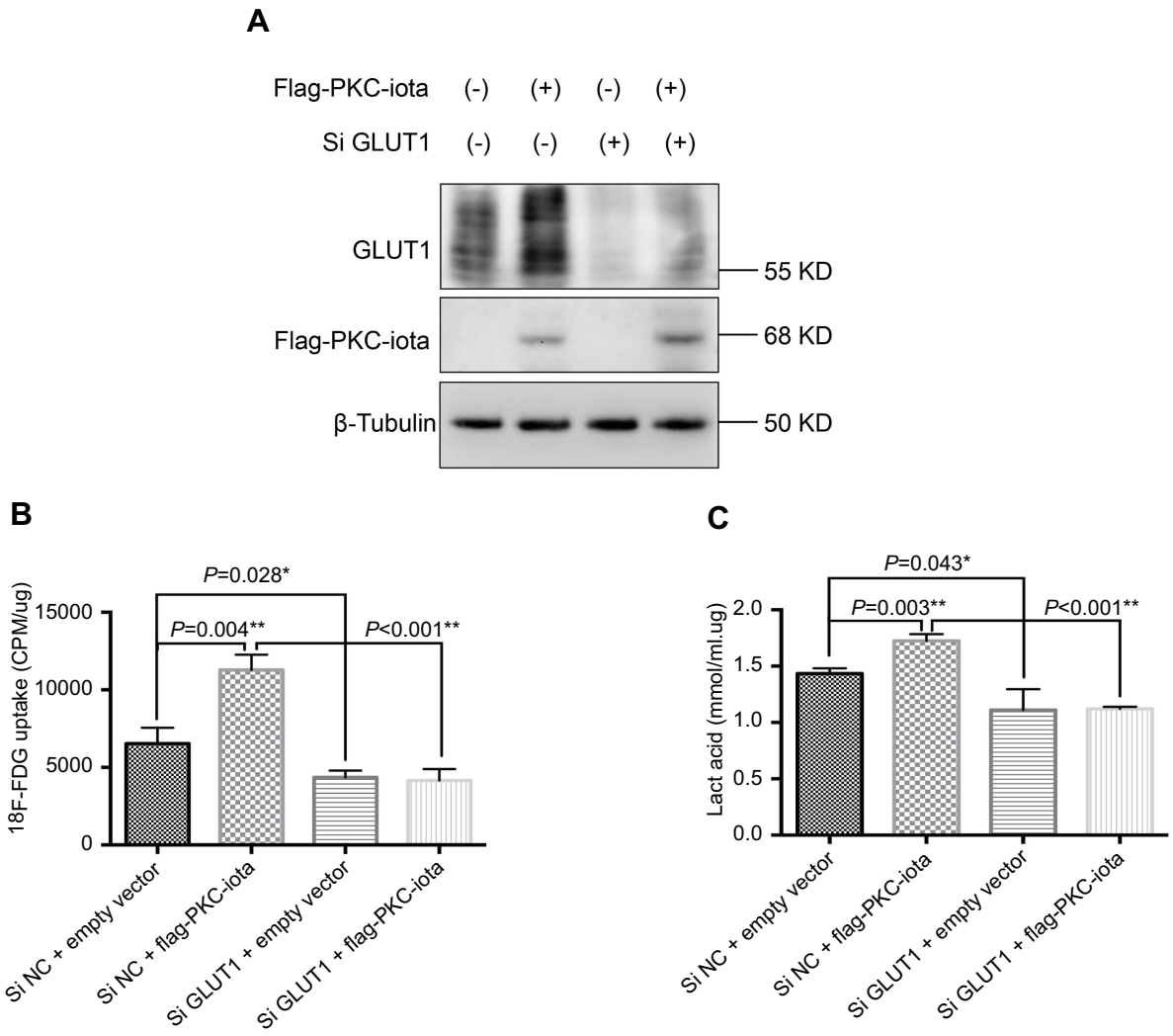

Figure 4 GLUT1 knockdown restrains PKC-iota-mediated ^{18}F-FDG uptake and glycolysis. (**A**) H1650 cells were co-transfected with Flag-PKC-iota (or empty vector) and Si GLUT1 (or Si NC) for 72 h. Cell lysates were immunoblotted with antibodies against GLUT1 and Flag, whereas β-tubulin was used as the loading control. (**B, C**) H1650 cells were co-transfected with Flag-PKC-iota (or empty vector) and Si GLUT1 (or Si NC) for 72 h, and then intracellular ^{18}F-FDG uptake (**B**) and lactification (**C**) were detected.

decrease in active, membrane-located GLUT1 induced by PKC-iota knockdown, which was also observed in our research, is the overall decrease in GLUT1 induced by c-Myc downregulation, which might differ from direct phosphorylation and activation of GLUT1 by other PKCs at the post-translational level.[14]

PKC-iota and GLUT1 overexpression in NSCLC were all essential for tumor progression,[30,31] which was also observed in our research; the protein levels of PKC-iota and GLUT1 were positively related to large tumor size, nodal metastasis, and late TNM stages. We also observed a positive relationship between PKC-iota and GLUT1 protein expression in NSCLC tissues, which could be reasonably explained by GLUT1 upregulation induced by PKC-iota. More importantly, cell growth assays showed that GLUT1 silencing suppressed PKC-iota-mediated cell proliferation, migration, and invasion, whereas IHC showed that NSCLC patients whose primary lesions showed high GLUT1 and PKC-iota co-expression had significantly worse survival than patients without PKC-iota and GLUT1 high co-expression. Taken together, these findings reasonably indicate the pivotal role of GLUT1-mediated glucose uptake and glycolysis in the PKC-iota-related progression of NSCLC.

In addition to being a well-characterized oncogenic enzyme, PKC-iota is also a promising target for tumor therapy, and clinical trials of PKC-iota inhibitors for NSCLC treatment are underway.[44,45] The positive correlation between PKC-iota and ^{18}F-FDG uptake in NSCLC

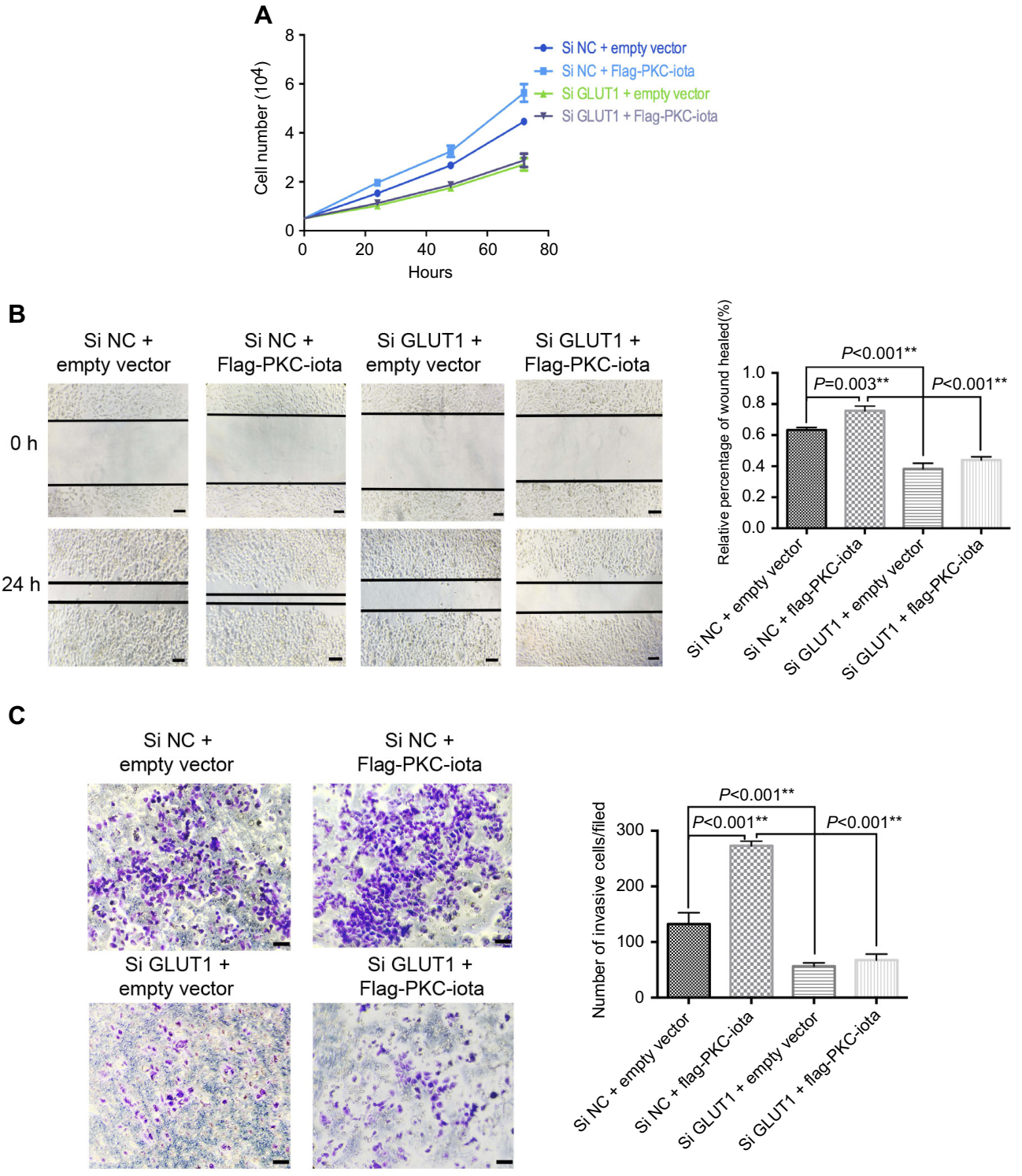

Figure 5 GLUT1 knockdown restrains PKC-iota-mediated growth of NSCLC cells. (**A**) After co-transfection with Flag-PKC-iota (or empty vector) and Si GLUT1 (or Si NC), the numbers of H1650 cells were counted at 24, 48, and 72 h. (**B, C**) H1650 cells were co-transfected with Flag-PKC-iota (or empty vector) and Si GLUT1 (or Si NC) for 36 h, after which time the cells were harvested to determine the migration and invasion capabilities by the wound-healing assay (left of (**B**) images of the indicated cells, scale bar: 25 μm; right of (**B**) statistical analysis of the migratory ability of the indicated cells) and transwell migration assay (left of (**C**) images of the indicated cells, scale bar: 25 μm; right of (**C**) statistical analysis of the invasive ability of the indicated cells), respectively.

indicates that ^{18}F-FDG PET/CT might be used to noninvasively quantify PKC-iota levels in NSCLC to guide ongoing clinical trials of anti-PKC-iota therapy. For cases in which tissue samples are unavailable for PKC-iota pathological testing,[46,47] ^{18}F-FDG PET/CT might predict PKC-iota levels in NSCLC, thus providing clues for anti-

Table 1 Correlation of PKC-iota and GLUT1 expression in 81 primary NSCLC tumor tissues with different clinicopathological parameters

Variable	Number	PKC-iota expression			GLUT1 expression		
		Low expression	High expression	*P*-value	Low expression	High expression	*P*-value
Age (years)							
≤60	24	9	15	0.402	12	12	0.084
>60	57	16	41		17	40	
Gender							
Female	23	9	14	0.310	9	14	0.694
Male	58	16	42		20	38	
Smoke							
Yes	57	16	41	0.402	23	34	0.188
No	24	9	15		6	18	
Pathological type							
SQCC	31	5	26	0.024*	6	25	0.015*
ADC	50	20	30		23	27	
Lesion length (cm)							
≤3	22	12	10	0.005*	14	8	0.001**
>3	59	13	46		15	44	
Nodal metastasis							
No	53	21	32	0.019*	24	29	0.014*
Yes	28	4	24		5	23	
TNM stage							
Stage I	38	18	20	0.003**	19	19	0.012*
Stage II-IV	43	7	36		10	33	

Notes: *P<0.05, **P<0.005.
Abbreviations: PKC-iota, protein kinase C-iota; GLUT1, glucose transporter 1; NSCLC, nonsmall cell lung cancer; SQCC, squamous carcinoma; ADC, adenocarcinoma.

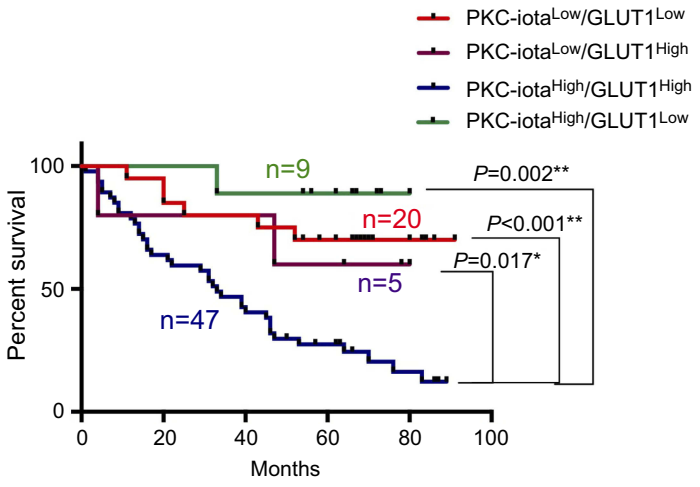

Figure 6 High PKC-iota and GLUT1 co-expression is related to poor NSCLC prognosis. Kaplan–Meier analysis of overall survival as a function of PKC-iota and GLUT1 levels in NSCLC tumor tissues.

PKC-iota treatment planning; patients whose tumor tissues strongly accumulate ^{18}F-FDG are more likely to benefit from anti-PKC-iota therapy than patients whose tumor lesions show relatively weak ^{18}F-FDG uptake. In addition, ^{18}F-FDG PET/CT can also be applied for monitoring the response to anti-PKC-iota drugs because a decrease in

^{18}F-FDG uptake decrease might indicate a positive anti-PKC-iota effect.

SQCC and ADC are the two main subtypes of NSCLC;[48] in NSCLC, SQCC always exhibits higher GLUT1-mediated glucose uptake and glycolysis levels than ADC.[49,50] In addition to GLUT1, a relatively high expression of PKC-iota in SQCC versus ADC was also observed in our study. The differences in ^{18}F-FDG uptake between SQCC and ADC might be explained by differences in PKC-iota-related GLUT1 activation in these two forms of NSCLC, which merits further research.

Conclusion

In conclusion, our data defined PKC-iota as a novel glycolysis-regulating enzyme in NSCLC, which is essential for tumor progression. PKC-iota promoted glucose uptake and glycolysis via upregulating c-Myc/GLUT1 signaling. PKC-iota inhibition might be a feasible and effective targeted strategy for the metabolic treatment of NSCLC. ^{18}F-FDG PET/CT might help predict PKC-iota status in NSCLC tissues, thus providing important clues for individualized anti-tumor therapy. In addition, the involvement of PKC-iota in tumor glucose metabolic reprogramming is expected to help identify new imaging agents not only for tumor diagnosis but also for therapeutic monitoring.

Acknowledgments

We thank Dr. Yuchen Han, PhD, (Shanghai Chest Hospital, Shanghai Jiaotong University) and Dr. Jinchen Shao, PhD, (Shanghai Chest Hospital, Shanghai Jiaotong University) for their assistance in immunohistochemical analysis. This study was supported by the National Natural Science Foundation of China (grant numbers 81602415, 81530053, & 81601524); the Natural Science Foundation of Shanghai (grant number 18ZR1435200); and the Scientific Research Project of Shanghai Municipal Commission of Health and Family Planning (grant number 20174Y0077).

Disclosure

The authors report no conflicts of interest in this work.

References

1. Miller KD, Siegel RL, Lin CC, et al. Cancer treatment and survivorship statistics, 2016. *CA Cancer J Clin*. 2016;66(4):271–289. doi:10.3322/caac.21349
2. Siegel RL, Miller KD, Jemal A. Cancer statistics, 2018. *CA Cancer J Clin*. 2018;68(1):7–30. doi:10.3322/caac.21442
3. Faubert B, Li KY, Cai L, et al. Lactate metabolism in human lung tumors. *Cell*. 2017;171(2):358–371e359. doi:10.1016/j.cell.2017.09.019
4. Yildirim F, Yurdakul AS, Ozkaya S, Akdemir UO, Ozturk C. Total lesion glycolysis by 18F-FDG PET/CT is independent prognostic factor in patients with advanced non-small cell lung cancer. *Clin Respir J*. 2017;11(5):602–611. doi:10.1111/crj.12391
5. Warburg O. [Origin of cancer cells]. *Oncologia*. 1956;9(2):75–83.
6. Ganapathy-Kanniappan S, Geschwind JF. Tumor glycolysis as a target for cancer therapy: progress and prospects. *Mol Cancer*. 2013;12:152. doi:10.1186/1476-4598-12-152
7. Newton AC. Protein kinase C: perfectly balanced. *Crit Rev Biochem Mol Biol*. 2018;53(2):208–230. doi:10.1080/10409238.2018.1442408
8. Fan C, Li Y, Jia J. Protein kinase Cs in lung cancer: a promising target for therapies. *J Cancer Res Ther*. 2013;9 Suppl 2:S74–79. doi:10.4103/0973-1482.119102
9. Isakov N. Protein kinase C (PKC) isoforms in cancer, tumor promotion and tumor suppression. *Semin Cancer Biol*. 2018;48:36–52. doi:10.1016/j.semcancer.2017.04.012
10. Regala RP, Weems C, Jamieson L, Copland JA, Thompson EA, Fields AP. Atypical protein kinase Ciota plays a critical role in human lung cancer cell growth and tumorigenicity. *J Biol Chem*. 2005;280(35):31109–31115. doi:10.1074/jbc.M505402200
11. Sarkar S, Bristow CA, Dey P, et al. PRKCI promotes immune suppression in ovarian cancer. *Genes Dev*. 2017;31(11):1109–1121. doi:10.1101/gad.296640.117
12. Troy A, Cadwallader AB, Fedorov Y, Tyner K, Tanaka KK, Olwin BB. Coordination of satellite cell activation and self-renewal by Par-complex-dependent asymmetric activation of p38alpha/beta MAPK. *Cell Stem Cell*. 2012;11(4):541–553. doi:10.1016/j.stem.2012.05.025
13. Rosse C, Lodillinsky C, Fuhrmann L, et al. Control of MT1-MMP transport by atypical PKC during breast-cancer progression. *Proc Natl Acad Sci U S A*. 2014;111(18):E1872–1879. doi:10.1073/pnas.1400749111
14. Siska PJ, Rathmell JC. PKCs sweeten cell metabolism by phosphorylation of Glut1. *Mol Cell*. 2015;58(5):711–712. doi:10.1016/j.molcel.2015.05.025
15. Szablewski L. Expression of glucose transporters in cancers. *Biochim Biophys Acta*. 2013;1835(2):164–169. doi:10.1016/j.bbcan.2012.12.004
16. Mueckler M, Thorens B. The SLC2 (GLUT) family of membrane transporters. *Mol Aspects Med*. 2013;34(2–3):121–138. doi:10.1016/j.mam.2012.07.001
17. Mueckle M. Facilitative glucose transporters. *Eur J Biochem*. 1994;219:713–725.
18. de Geus-Oei LF, van Krieken JH, Aliredjo RP, et al. Biological correlates of FDG uptake in non-small cell lung cancer. *Lung Cancer*. 2007;55(1):79–87. doi:10.1016/j.lungcan.2006.08.018
19. Zhao FQ, Keating AF. Functional properties and genomics of glucose transporters. *Curr Genomics*. 2007;8(2):113–128.
20. Fenske W, Volker HU, Adam P, et al. Glucose transporter GLUT1 expression is an stage-independent predictor of clinical outcome in adrenocortical carcinoma. *Endocr Relat Cancer*. 2009;16(3):919–928. doi:10.1677/ERC-08-0211
21. Liu Y, Cao Y, Zhang W, et al. A small-molecule inhibitor of glucose transporter 1 downregulates glycolysis, induces cell-cycle arrest, and inhibits cancer cell growth in vitro and in vivo. *Mol Cancer Ther*. 2012;11(8):1672–1682. doi:10.1158/1535-7163.MCT-12-0131
22. Kaira K, Serizawa M, Koh Y, et al. Relationship between 18F-FDG uptake on positron emission tomography and molecular biology in malignant pleural mesothelioma. *Eur J Cancer*. 2012;48(8):1244–1254. doi:10.1016/j.ejca.2012.01.016
23. Ganapathy V, Thangaraju M, Prasad PD. Nutrient transporters in cancer: relevance to Warburg hypothesis and beyond. *Pharmacol Ther*. 2009;121(1):29–40. doi:10.1016/j.pharmthera.2008.09.005
24. Ohno H, Nakatsu Y, Sakoda H, et al. 4F2hc stabilizes GLUT1 protein and increases glucose transport activity. *Am J Physiol Cell Physiol*. 2011;300(5):C1047–1054. doi:10.1152/ajpcell.00416.2010

25. Guo Z, Jia J, Yao M, et al. Diacylglycerol kinase gamma predicts prognosis and functions as a tumor suppressor by negatively regulating glucose transporter 1 in hepatocellular carcinoma. *Exp Cell Res*. 2018;373(1–2):211–220. doi:10.1016/j.yexcr.2018.11.001
26. Li L, Liang Y, Kang L, et al. Transcriptional regulation of the warburg effect in cancer by SIX1. *Cancer Cell*. 2018;33(3):368–385e367. doi:10.1016/j.ccell.2018.01.010
27. Osthus RC, Shim H, Kim S, et al. Deregulation of glucose transporter 1 and glycolytic gene expression by c-Myc. *J Biol Chem*. 2000;275(29):21797–21800. doi:10.1074/jbc.C000023200
28. Riddell M, Nakayama A, Hikita T, et al. aPKC controls endothelial growth by modulating c-Myc via FoxO1 DNA-binding ability. *Nat Commun*. 2018;9(1):5357. doi:10.1038/s41467-018-07739-0
29. Bomanji JB, Costa DC, Ell PJ. Clinical role of positron emission tomography in oncology. *Lancet Oncol*. 2001;2(3):157–164.
30. Luo Q, Tang L, Lin H, et al. The oncogenic role of PKCiota gene amplification and overexpression in Chinese non-small cell lung cancer. *Lung Cancer*. 2014;84(2):190–195. doi:10.1016/j.lungcan.2013.08.029
31. Tan Z, Yang C, Zhang X, Zheng P, Shen W. Expression of glucose transporter 1 and prognosis in non-small cell lung cancer: a pooled analysis of 1665 patients. *Oncotarget*. 2017;8(37):60954–60961. doi:10.18632/oncotarget.17604
32. Yan YF, Zheng YF, Ming PP, Deng XX, Ge W, Wu YG. Immune checkpoint inhibitors in non-small-cell lung cancer: current status and future directions. *Brief Funct Genomics*. 2019;18(2):147–156. doi:10.1093/bfgp/ely029
33. Sequist LV, Martins RG, Spigel D, et al. First-line gefitinib in patients with advanced non-small-cell lung cancer harboring somatic EGFR mutations. *J Clin Oncol*. 2008;26(15):2442–2449. doi:10.1200/JCO.2007.14.8494
34. Pakkala S, Ramalingam SS. Personalized therapy for lung cancer: striking a moving target. *JCI Insight*. 2018;3(15). doi:10.1172/jci.insight.97941
35. Nakamura H, Saji H, Marushima H, et al. Standardized uptake values in the primary lesions of non-small-cell lung cancer in FDG-PET/CT can predict regional lymph node metastases. *Ann Surg Oncol*. 2015;22 Suppl 3:S1388–1393. doi:10.1245/s10434-015-4564-6
36. Calandriello L, Larici AR, Leccisotti L, et al. Multifunctional assessment of non-small cell lung cancer: perfusion-metabolic correlation. *Clin Nucl Med*. 2018;43(1):e18–e24. doi:10.1097/RLU.0000000000001888
37. Lapa P, Oliveiros B, Marques M, et al. Metabolic tumor burden quantified on [(18)F]FDG PET/CT improves TNM staging of lung cancer patients. *Eur J Nucl Med Mol Imaging*. 2017;44(13):2169–2178. doi:10.1007/s00259-017-3789-y
38. Justilien V, Walsh MP, Ali SA, Thompson EA, Murray NR, Fields AP. The PRKCI and SOX2 oncogenes are coamplified and cooperate to activate Hedgehog signaling in lung squamous cell carcinoma. *Cancer Cell*. 2014;25(2):139–151. doi:10.1016/j.ccr.2014.01.008
39. Atwood SX, Li M, Lee A, Tang JY, Oro AE. GLI activation by atypical protein kinase C iota/lambda regulates the growth of basal cell carcinomas. *Nature*. 2013;494(7438):484–488. doi:10.1038/nature11889
40. Linch M, Sanz-Garcia M, Rosse C, et al. Regulation of polarized morphogenesis by protein kinase C iota in oncogenic epithelial spheroids. *Carcinogenesis*. 2014;35(2):396–406. doi:10.1093/carcin/bgt313
41. Fields AP, Regala RP. Protein kinase C iota: human oncogene, prognostic marker and therapeutic target. *Pharmacol Res*. 2007;55(6):487–497.
42. Wang Y, Justilien V, Brennan KI, Jamieson L, Murray NR, Fields AP. PKCiota regulates nuclear YAP1 localization and ovarian cancer tumorigenesis. *Oncogene*. 2017;36(4):534–545. doi:10.1038/onc.2016.224
43. Dejure FR, Eilers M. MYC and tumor metabolism: chicken and egg. *Embo J*. 2017;36(23):3409–3420. doi:10.15252/embj.201796438
44. Fields AP, Ali SA, Justilien V, Murray NR. Targeting oncogenic protein kinase Ciota for treatment of mutant KRAS LADC. *Small GTPases*. 2017;8(1):58–64. doi:10.1080/21541248.2016.1194953
45. Mansfield AS, Fields AP, Jatoi A, et al. Phase I dose escalation study of the PKCiota inhibitor aurothiomalate for advanced non-small-cell lung cancer, ovarian cancer, and pancreatic cancer. *Anticancer Drugs*. 2013;24(10):1079–1083. doi:10.1097/CAD.0000000000000009
46. Lindeman NI, Cagle PT, Beasley MB, et al. Molecular testing guideline for selection of lung cancer patients for EGFR and ALK tyrosine kinase inhibitors: guideline from the College of American Pathologists, International Association for the Study of Lung Cancer, and Association for Molecular Pathology. *J Mol Diagn*. 2013;15(4):415–453. doi:10.1016/j.jmoldx.2013.03.001
47. Gerlinger M, Rowan AJ, Horswell S, et al. Intratumor heterogeneity and branched evolution revealed by multiregion sequencing. *N Engl J Med*. 2012;366(10):883–892. doi:10.1056/NEJMoa1113205
48. Mountain CF, Lukeman JM, Hammar SP, et al. Lung cancer classification: the relationship of disease extent and cell type to survival in a clinical trials population. *J Surg Oncol*. 1987;35(3):147–156.
49. Goodwin J, Neugent ML, Lee SY, et al. The distinct metabolic phenotype of lung squamous cell carcinoma defines selective vulnerability to glycolytic inhibition. *Nat Commun*. 2017;8:15503. doi:10.1038/ncomms15503
50. Koh YW, Lee SJ, Park SY. Differential expression and prognostic significance of GLUT1 according to histologic type of non-small-cell lung cancer and its association with volume-dependent parameters. *Lung Cancer*. 2017;104:31–37. doi:10.1016/j.lungcan.2016.12.003

Supplementary material

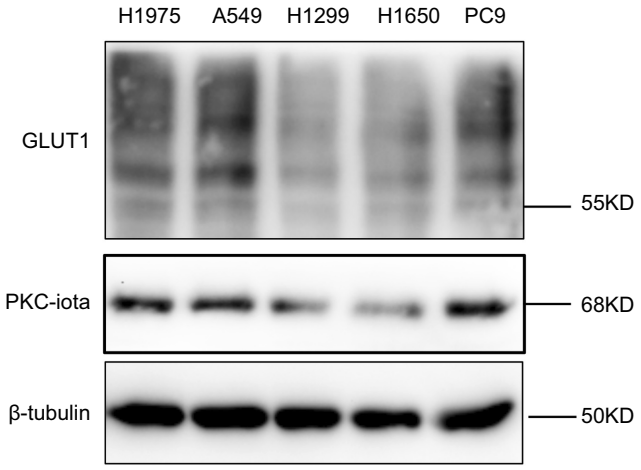

Figure S1 The basal protein levels of GLUT1 and PKC-iota in NSCLC cell lines. NSCLC cells lysates were immunoblotted with indicated antibodies. β-Tubulin served as the loading control.